Rh nanoparticles confined in triphenylphosphine oxide-functionalized core-crosslinked micelles with a polyanionic shell: Synthesis, characterization, and application in aqueous biphasic hydrogenation

Chantal Abou-Fayssal, Leonhard Schill, Rinaldo Poli, Anders Riisager, Eric Manoury, Karine Philippot

Rh nanoparticles confined in triphenylphosphine oxide-functionalized core-crosslinked micelles with a polyanionic shell: synthesis, characterization, and application in aqueous biphasic hydrogenation

Chantal J. Abou-Fayssal,[a,b] Leonhard Schill,[b] Rinaldo Poli,[*b,c] Anders Riisager,[*a] Eric Manoury,[*b] Karine Philippot[*b]

[a] *Centre for Catalysis and Sustainable Chemistry, Department of Chemistry, Technical University of Denmark, Kemitorvet, Building 207, 2800 Kgs. Lyngby, Denmark.*
[b] *CNRS, LCC (Laboratoire de Chimie de Coordination), Université de Toulouse, UPS, INP, 205 route de Narbonne, BP 44099, F-31077 Toulouse Cedex 4, France.*
[c] *Institut Universitaire de France, 1, rue Descartes, 75231 Paris Cedex 05, France.*

Abstract

Core-crosslinked micelles (CCMs) with a hydrophilic polyanionic shell made of poly(sodium styrene sulfonate) chains, P(SS^-Na^+), a triphenylphosphine oxide-functionalized polystyrene core (TPPO@PSt) and crosslinked at the inner end of the polystyrene chains by diethylene glycol dimethacrylate (DEGDMA) were synthesized by reversible addition-fragmentation chain-transfer (RAFT) polymerization as a stable TPPO@CCM-A latex. One-pot synthesis of rhodium nanoparticles (RhNPs) by the reduction of $[Rh(COD)(\mu\text{-}Cl)]_2$ in the aqueous TPPO@CCM-A latex yielded a stable RhNP-TPPO@CCM-A latex without the need of additional stabilizer or base. This Rh-loaded latex was applied to the catalytic biphasic hydrogenation of styrene under mild conditions with complete selectivity towards ethylbenzene and corrected turnover frequencies (*c*TOFs) ranging from 3250 to 10010 h^{-1} based on the surface atoms of the RhNPs. Importantly, the catalytic phase proved recyclable after product extraction, owing to the efficient retention of the RhNPs by the core TPPO ligands.

Keyword. Rhodium nanoparticles - Polymeric nanoreactors - Aqueous biphasic hydrogenation catalysis – Styrene

1. Introduction

Catalysis with well-defined metal nanoparticles (MNPs) [1,2] is a bridge between homogeneous and heterogeneous catalysis. The nanometric dimension of MNPs provides distinctive properties not attainable with conventional bulk materials, thereby allowing for specific reactivity and advantageous properties including high efficiency, selectivity, stability, and ease of recovery/recycling [3–6]. Multiple methods have been developed for the synthesis of RhNPs based on the reduction of metal salts and low-valent organometallic Rh precursors [7,8]. Typically, size control is achieved by adding capping agents in the synthesis medium, *e.g.* surfactants (ammonium salts) [9–11], polymers [12–15], dendrimers [5] or ligands [7,16–22], which limit the growth of the RhNPs and ensure their stabilization in solution. The capping agents can also facilitate the recovery and recycling of the NPs, a key point for developing applications in catalysis.

Aqueous biphasic catalysis can be performed with polymer-supported RhNPs, where the polymers form a stable colloidal dispersion in the aqueous medium [23–25] and the RhNPs are anchored to the hydrophobic cores of the polymer micelles. These systems provide easy catalyst recovery and recycling by simple phase separation. Some of us have developed efficient protocols to prepare highly modular core-crosslinked micelles (CCMs) [26–35] as stable aqueous dispersions with a high polymer content (> 20 wt%), by reversible addition-fragmentation chain-transfer (RAFT) polymerization [36]. The first generation of CCMs designed contained a neutral shell (CCM-N) made of random copolymer blocks of poly(ethylene oxide) (PEO) methacrylate and methacrylic acid [27]. Then, a second generation of analogous CCMs with a polycationic shell (CCM-C) of homopolymer blocks of 4-vinyl-*N*-methylpyridinium iodide (4VPMe$^+$I$^-$) was reported [28]. Both CCM-N and CCM-C had a polystyrene-based core with diethylene glycol dimethacrylate (DEGDMA) as crosslinker but were functionalized with different phosphine-based core-linked ligands (L@CCM), where L = triphenylphosphine (TPP), bis(4-methoxyphenyl)phenyl-phosphine [37], nixantphos [27], or triphenylphosphine oxide (TPPO) [34,35].

Recently, a third generation of CCMs with a polyanionic shell (CCM-A) of homopolymer blocks of poly(sodium styrene sulfonate) has also been developed [28,38]. The CCM-A system requires fewer synthetic steps for its preparation than

CCM-C and has, compared to CCM-N systems, the advantage of improved phase separation in aqueous biphasic hydrogenation as the charged nature of the outer shell prevents core-crosslinked micelle interpenetration owing to the repulsion induced by Coulombic forces. However, when the CCM-A micelles were used as nanoreactors for the confinement of a molecular Rh pre-catalyst [38], the interaction of the latter with the polyanionic shell prevented effective catalyst loading. Note that a similar problem has also occurred for neutral shell micelles with ionizable carboxylic acid functions [39].

In this work, we report the synthesis of a TPPO@CCM-A polymer as a latex by RAFT polymerization. This new polymer was further used to prepare a RhNP-TPPO@CCM-A latex by a one-pot synthesis entailing the reduction of $[Rh(COD)(\mu\text{-}Cl)]_2$, vectorized by toluene, in the presence of the TPPO@CCM-A latex without requiring auxiliary stabilizer or base. The RhNP-TPPO@CCM-A latex proved effective and recyclable in the aqueous biphasic hydrogenation of both styrene and acetophenone.

2. Experimental

2.1. Material and Methods

Unless otherwise stated, all experiments were carried out using Schlenk-line techniques under an inert atmosphere of dry argon. (4-Styryl)diphenylphosphine (SDPP, 97%, Aldrich), 4,4'-azobis(4-cyanopentanoic acid) (ACPA, >98%, Fluka), diethylene glycol dimethacrylate (DEGDMA, 95%, Sigma-Aldrich), sodium 4-vinylbenzenesulfonate (SS^-Na^+, >90%, Aldrich), $[Rh(COD)(\mu\text{-}Cl)]_2$ (>98%, Sigma-Aldrich) and hydrogen (99.999%, Air Liquide) were used as received. Styrene (St, 99%, Acros) was distilled under reduced pressure prior to use. The RAFT agent 4-cyano-4-thiothiopropylsulfanyl pentanoic acid (CTPPA) or R_0-SC(S)S*n*Pr (R_0 = $C(CH_3)(CN)CH_2CH_2COOH$) [30] and the R_0-$(SS^-Na^+)_{140}$-SC(S)S*n*Pr and R_0-$(SS^-Na^+)_{140}$-*b*-St_{50}-SC(S)S*n*Pr macroRAFT agents (the number of monomer units indicated in the formula are average degrees of polymerization) were synthesized as previously described [28]. (4-Styryl)diphenylphosphine oxide (SDPPO) was synthesized following a literature procedure [40]. The deionized water used for the polymer syntheses and the characterization were obtained using a Purelab Classic

UV system (Elga Lab-Water). The autoclaves used for the syntheses of RhNPs and the hydrogenation catalysis were homebuilt (volume 15 mL).

2.2. Characterization

2.2.1. Dynamic light scattering (DLS)

The z-average diameters of the polymer core cross-linked micelles (Dz) and the polydispersity index (PDI) were obtained with a Malvern Zetasizer NanoZS equipped with a He-Ne laser (λ = 633 nm), operating at 23 °C. Samples were analyzed after dilution (with deionized water), either unfiltered or after filtration through a 0.45 µm pore-size membrane. The procedure without filtration allowed verification of the presence of agglomerates. Each reported value is the average of five measurements and figure data labeled N, V and I represent the instrumental responses in number, volume, and intensity, respectively.

2.2.2. Transmission electron microscopy (TEM)

Morphological analyses of polymer core cross-linked micelles and RhNPs were carried out with a JEOL JEM 1400 transmission electron microscope working at 120 kV (Centre de Microcaractérisation Raimond Castaing, UAR 3623, Toulouse, France). Diluted aqueous samples were dropped on a formvar/carbon-coated copper grid and dried under vacuum for 24 h before measurements.

2.2.3. Gas chromatography (GC)

Quantitative determination of products and residual substrates in organic phases after catalysis was conducted with an Agilent 6890N gas chromatograph equipped with an HP-5MS capillary column (30 m × 250 µm × 0.25 µm) and a flame ionization detector (FID), using helium as carrier gas. The peak assignment was assisted by separate GC mass spectrometry (GC-MS) analysis using an Agilent 6850-5975C.

2.2.4. Inductive coupled plasma mass spectrometry (ICP-MS)

Rh metal leaching into the organic phase after catalysis was quantified by high-resolution ICP-MS using an XR Thermo Scientific Element. For the sample preparation, the recovered organic phase was diluted in water using a 104 volumetric dilution factor, high enough to ensure complete dissolution. In practice, a 100 mL volumetric flask was filled 2/3 with Milli-Q water, then 10 µl of the organic product

phase was introduced using a precision pipette. The borders were rinsed, and the flask was introduced into an ultrasound bath for 15 min. The dilution was then completed with Milli-Q water to the 100 mL mark, followed by further sonication for 45 min. Standards were prepared using [Rh(COD)(μ-Cl)]$_2$ dissolved in toluene, attaining Rh concentrations in aqueous solution in the 1-100 ppt range. The relative standard deviation on the measurements used for the calibration was 3%.

2.2.5. X-ray photoelectron spectroscopy (XPS)

XPS analyses were performed using a Thermo Scientific system at room temperature using AlKα radiation (1484.6 eV) and a spot size of 400 μm. A flood gun was used to reduce sample charging effects and the obtained spectra were further corrected by setting the C1s binding energy at 284.8 eV. Data processing was done using the Avantage 5.948 software.

2.2.6. Thermo gravimetric analysis (TGA) and differential scanning calorimetry (DSC)

TGA and DSC measurements were carried out on a Mettler Toledo TGA/DSC 3+ instrument under a N_2 flow. Samples were placed into an alumina crucible and then heated from room temperature to 800 °C at a heating rate of 10 °C min^{-1}.

2.2.7. Fourier-transform infrared spectroscopy (FTIR)

FTIR spectra of freeze-dried samples were measured using a PerkinElmer Spectrum 100 FT-IR spectrometer equipped with diamond attenuated total reflectance (ATR) mode. Each measurement consisted of an average of two scans (600–4000 cm^{-1}) with background correction.

2.3. Synthesis

2.3.1. Preparation of a latex of the R$_0$-(SS$^-$Na$^+$)$_{140}$-*b*-St$_{50}$-*b*-(St$_{0.9}$-*co*-SDPPO$_{0.1}$)$_{300}$-SC(S)S*n*Pr amphiphilic triblock copolymers

The latex synthesis followed the same procedure as the analogous phosphine-functionalized systems reported in the literature [28,38]. To the pale-yellow latex of the R$_0$-(SS$^-$Na$^+$)$_{140}$-*b*-St$_{50}$-SC(S)S*n*Pr macroRAFT agent (0.04 mmol of polymer, corresponding to 0.56 mmol of SS$^-$Na$^+$ units, 3 mL of water) were added degassed styrene (1.24 mL, 1.12 g, 10.75 mmol; 270 equiv. per chain), SDPPO (0.34 g, 1.20 mmol; 30 equiv. per chain) and trioxane (ca. 90 mg) as an internal standard. A portion

of a degassed ACPA/$NaHCO_3$ stock solution (0.11 mL, 2.2 mg ACPA, 7.96 µmol) was then added and the resulting reaction mixture was stirred at 80 °C for 4.5 h, yielding a white opalescent stable dispersion. The resulting polymer has a theoretical molar mass of 66869 g mol^{-1}. Polymer content in latex = 18.8 wt%.

2.3.2. Preparation of a latex of of the R_0-(SS^-Na^+)$_{140}$-*b*-St_{50}-*b*-($St_{0.9}$-*co*-$SDPPO_{0.1}$)$_{300}$-SC(S)S*n*Pr core-crosslinked micelles (TPPO@CCM-A)

To the total volume of a R_0-(SS^-Na^+)$_{140}$-*b*-St_{50}-*b*-($St_{0.9}$-*co*-$SDPPO_{0.1}$)$_{300}$-SC(S)S*n*Pr latex obtained as described above (0.04 mmol of polymer) were successively added DEGDMA (0.13 mL, 144.3 mg, 0.60 mmol; 15 equiv. per chain), styrene (0.62 mL, 561.6 mg, 5.4 mmol; 135 equiv. per chain) and a degassed ACPA/$NaHCO_3$ stock aqueous solution (0.11 mL, 2.2 mg ACPA, 7.96 µmol). The resulting reaction mixture was then stirred at 80 °C for 4 h leading to complete co-monomer consumption (^{1}H NMR monitoring in DMSO-d_6) and yielding the CCM R_0-(SS^-Na^+)$_{140}$-*b*-St_{50}-*b*-($St_{0.9}$-*co*-$SDPPO_{0.1}$)$_{300}$-*b*-($DEGDMA_{0.1}$-*co*-$St_{0.9}$)$_{150}$-SC(S)S*n*Pr. Polymer content = 14.4 wt%, [TPPO] = 65.3 µmol mL^{-1}.

2.3.3. One-pot synthesis of RhNP-TPPO@CCM-A latex

A TPPO@CCM-A latex (6 mL, 71.3 µmol of P=O ligands) was stirred (1200 rpm) for 15 min after the addition of toluene (8 mL) to swell the CCM cores. Afterward, a toluene solution (3.2 mL) with [Rh(COD)(*µ*-Cl)]$_2$ (6.2 mg, 12.2 µmol) was added and the mixture was stirred (1200 rpm) for another 5 min before being transferred to a glass vial (40 x 20 mm), which was placed into an autoclave. The autoclave was then charged with 20 bar of H_2 and positioned in an aluminum heating block at 60 °C and stirred (1200 rpm) for 20 h. After reaction the autoclave was carefully depressurized and after simple separation from the colorless and transparent toluene phase (top), the nanocatalyst was recovered as a black latex phase (bottom) and used directly for catalysis.

2.4. Catalysis

2.4.1. Aqueous biphasic hydrogenation with RhNP-TPPO@CCM-A latex

To a glass vial containing the RhNP-TPPO@CCM-A latex (0.5 mL, 5.9 µmol of P=O ligands, 2.5 µmol of metal) were added the desired amounts of styrene or acetophenone (5.0 or 12.5 mmol) and decane (internal standard; substrate/internal

standard molar ratio *ca*. 4). The vial was then placed inside an autoclave, which was charged with 20 bar of H_2 and placed in an aluminum heating block at a desired temperature between 24-60 °C with magnetic stirring (1200 rpm) for a reaction time of up to 2 h. After the set time, the stirring was stopped, the autoclave slowly vented and the vial removed (under argon), whereafter the reaction mixture was left standing to allow phase separation. After complete phase separation, the latex was extracted with diethyl ether (3 × 0.3 mL), applying 5 min of stirring (1200 rpm) followed by 5 min of phase separation without stirring for each extraction (operations carried out in air). Lastly, the combined organic phases were analyzed by GC.

2.4.2. Catalyst recycling experiments

After product separation, the vial containing the RhNP-TPPO@CCM-A latex from the previous hydrogenation run was charged with fresh substrate (same amount as in the initial run), followed by reaction and product separation procedures according to the protocols described above.

3. Results and Discussion

3.1. Polymer Synthesis and Characterization

The TPPO@CCM-A was synthesized by the convergent strategy optimized for the preparation of the other CCMs [28,38], with the α- and ω-chain ends of the micellar arms provided by the RAFT chain transfer agent CTPPA. The optimized synthesis of CCM-A was reported previously using SDPP as core monomer in RAFT polymerization, while the use of SDPPO for the synthesis of a CCM-C was described more recently [34]. The final latexes that contain up to 14.4 wt% of polymer, showed the expected low viscosity for a suspension of spherical micelles (i.e., not very different from water alone) and proved stable over several months with no evidence of coagulation.

The average degrees of polymerization were fixed to 140 for the outer hydrophilic P(SS^-Na^+) shell and 300+50 for the polystyrene (PSt) core (Scheme 1). The fraction of SDPPO (a solid monomer) in the St/SDPPO mixture was limited by the SDPPO solubility in styrene (*ca.* 25 mol%). CCMs were initially developed by extending the R_0-(SS^-Na^+)$_{140}$-SC(S)S*n*Pr macromolecules with a short PSt block (50 monomer units),

yielding an amphiphilic diblock copolymer, which self-assembles (Step 2). Further chain extension of the R_0-(SS^-Na^+)$_{140}$-*b*-St_{50}-SC(S)S*n*Pr macroRAFT agent with the St/SDPPO (90/10) mixture was performed directly as an emulsion polymerization, ensuring full incorporation of the SDPPO monomer in the CCM core as confirmed by ^{1}H NMR (SI, Figure S1), and leading to R_0-(SS^-Na^+)$_{140}$-*b*-St_{50}-*b*-($St_{0.9}$-*co*-*S*$DPPO_{0.1}$)$_{300}$-SC(S)S*n*Pr (Step 3). The spherical micelles of the amphiphilic diblock copolymer thus produced in step 4 had an average size of *ca.* 32 nm, as shown by DLS analysis (Figure 1a). The final crosslinking step was carried out with DEGDMA (15 equiv. per chain) diluted with additional styrene (135 equiv. per chain), leading to complete monomer consumption and generation of CCM-A of composition R_0-(SS^-Na^+)$_{140}$-*b*-St_{50}-*b*-($St_{0.9}$-*co*-*S*$DPPO_{0.1}$)$_{300}$-*b*-($St_{0.9}$-*co*-$DEGDMA_{0.1}$)$_{150}$-SC(S)S*n*Pr (Step 4), with a 10% crosslink density in the inner crosslinked core (^{1}H NMR in SI, Figure S2).

<Scheme 1>

The final TPPO@CCM-A polymer core-crosslinked micelles had a spherical morphology and a slightly larger diameter (45 nm) than the intermediate micelles, as shown by DLS (Figure 1b) and TEM (Figure 1d) analyses. Also, they were smaller than their analogs synthesized in the presence of SDPP (~130 nm) [38]. After swelling with $CHCl_3$ (Figure 1c), the size distribution was relatively unchanged which can be attributed to the dominant effect of micelle disaggregation as also seen before with TPP@CCM-A [28,38] as well as TPP@CCM-C [29] and TPPO@CCM-C [34,35].

<Figure 1>

3.2. Synthesis and Characterization of RhNPs-TPPO@CCM-A

A stable latex of RhNP-TPPO@CCM-A was straightforwardly synthesized in a single step by heating (60 °C) a biphasic mixture containing the TPPO@CCM-A latex and a toluene solution of [Rh(COD)(*μ*-Cl)]$_2$ under H_2 (20 bar), without any additive (auxiliary stabilizer or base). The obtained latex (bottom) was black while the toluene phase (top) was colorless and transparent, signaling the successful formation and confinement of RhNPs in the CCM-A cores. A TEM analysis of the obtained RhNP-TPPO@CCM-A latex evidenced the polymer core loading with RhNPs, which displayed a mean size of 3.1 ± 0.6 nm (Figure 2).

<Figure 2>

The stability of the RhNP-TPPO@CCM-A was studied by TGA under N_2 (SI, Figure S2). The results indicated a temperature of decomposition (T_{dec}) of 254 °C followed by a gradual weight loss of 60 wt% at 418 °C, attributed to the total decomposition of the polymeric chains.

The interaction between the polymer and the RhNPs was further analyzed by XPS (SI, Figures S4-S7). XPS results revealed a shift in the TPPO binding energy after RhNP loading, which was particularly noticeable for the O 1s excitation (ΔE = 0.8 eV (Scan A) and 0.99 eV (Scan B), SI Table S1) and less distinct for the other elements. The pronounced O 1s binding energy shift agrees with the presence of Rh-O interactions between the RhNPs and the TPPO@CCM-A polymer, as also previously reported for RhNP-TPPO@CCM-C [34]. For comparison, RhNPs were also synthesized in the presence of TPPO (Rh/TPPO = 1/4) alone and characterized using XPS. The Rh binding energy shift between RhNP-TPPO and RhNP-TPPO@CCM-A tended here towards zero (SI, Table S2), suggesting a comparable interaction between RhNPs and TPPO as a free ligand and TPPO in the micelles, thus implying that the coordination most likely occurs with the TPPO of the micelles.

The ATR-FTIR spectra of TPPO@CCM-A and RhNP-TPPO@CCM-A were also compared to that of pristine TPPO [34]. The strong P=O stretching band of TPPO (1178 cm^{-1}) [41] was well visible in TPPO@CCM-A but being less intense and appeared slightly blue-shifted (~1181 cm^{-1}) in RhNP-TPPO@CCM-A (SI, Figure S8). In comparison, the shift was more pronounced and red-shifted (~1156 cm^{-1}) for RhNP-TPPO@CCM-C [35,42,43]. Given that the cores of CCM-A and CCM-C are similar, this might indicate that the interaction between the TPPO@CCM-A and the RhNPs are different than previously observed with TPPO@CCM-C.

To further investigate the RhNP-polymer interaction, a TPPO-free CCM-A, and a corresponding RhNP@CCM-A latex were synthesized following a previously optimized procedure [28] and the single-step procedure described for RhNP-TPPO@CCM-A (*vide supra*). The TEM analysis of RhNP@CCM-A showed the presence of somewhat agglomerated RhNPs (SI, Figure S9), whereas the FTIR-ATR spectrum of the polymer (SI, Figure S8) showed more intense aromatic C-H stretching

bands (1494 and 1450 cm^{-1}) than observed for RhNP-TPPO@CCM-A. XPS analyses of the RhNP@CCM-A also revealed increased shift in binding energy of the O1s excitation (ΔE = 1.9 eV (Scan A) and 2.03 eV (Scan B)) (SI, Table S3) compared to that observed for the RhNP-TPPO@CCM-A (*vide supra*). These results corroborate the presence of interactions of different natures between the RhNPs and the TPPO@CCM-A besides those with the TPPO core ligands. Such interactions may [k1]include coordination to the P(SS^-Na^+) shell *via* the thiocarbonic diester groups as such moieties are expected to be good ligands for Rh^0.

3.3. Hydrogenation Catalysis with RhNP-TPPO@CCM-A

3.3.1. Styrene hydrogenation

The hydrogenation of styrene (St) with the RhNP-TPPO@CCM-A latex was performed under 20 bar H_2 pressure for 0.25 h at temperatures of 24-37 °C using St/Rh ratios of 2000/1 or 5000/1 under a high stirring rate (1200 rpm) (Table 1). The high stirring speed limited external mass transport, which proved dominating at lower stirring rates. The latex proved active yielding styrene conversion up to 54% at 37 °C with a St/Rh ratio of 2000/1 (Table 1, Entry 4), corresponding to an average TOF value of 4375 h^{-1} (*c*TOF value of 10010 h^{-1}). In addition, an excellent selectivity (>99 %) towards ethyl benzene (EB) was achieved with less than 0.1 % hydrogenation of the aromatic ring to ethyl cyclohexane (ECH). A series of experiments conducted with a St/Rh ratio of 2000/1 at 25 °C and longer reaction times evidenced full styrene conversion (>99 %) after 2 h, corresponding to an average TOF of 1100 h^{-1} (*c*TOF of 2500 h^{-1}), still with >99 % selectivity towards EB (Figure 3).

<Table 1>

<Figure 3>

The excellent selectivity achieved towards EB using both the RhNP-TPPO@CCM-A latex (mean size of RhNPs of 3.1 ± 0.6 nm, *c*TOF up to 10010 h^{-1}) and its analogous RhNP-TPPO@CCM-C latex (mean size of RhNPs of 1.7 ± 0.2 nm, *c*TOF up to 23,600 h^{-1}) [34,35] denotes that the selectivity is independent of the RhNP size as well as the outer CCM shell nature (cationic or anionic) and size (44 and 98 nm, respectively). However, as previous works [32,34] showed that both the nature of the core

crosslinked micelles and the coordinating ligands of RhNPs can alter the selectivity in styrene hydrogenation, determining the impact of the NP surface coverage could motivate future investigations with different core anchoring ligands.

The apparent activation energies *(E_a)* of the reactions conducted with the RhNPs-TPPO@CCM-A latex at St/Rh ratios of 2000/1 and 5000/1 were estimated *via* Arrhenius plots (SI, Figures S10 and S11). The E_a obtained for a St/Rh ratio of 5000/1 in the 24-31 °C range (30 ± 0.5 kJ mol^{-1}; Table 1, Entries 5-7) is significantly lower than that determined for the analogous reaction conducted with RhNP-TPPO@CCM-C (69 ± 6 kJ mol^{-1}) [35]. This result points to more severe mass transport limitation with the RhNP-TPPO@CCM-C catalytic system. Conversely, the E_a was estimated as 82 ± 0.5 kJ mol^{-1} for the reaction with a St/Rh ratio of 2000/1 in the same temperature range (Table 1, Entries 1-3). It is likely that the mass transport limitation with the St/Rh ratio of 5000/1 arises, at least partially, from the significantly higher volume of substrate used (St/latex volume ratio *ca.* 2), compared to that introduced with the St/Rh ratio of 2000/1. Moreover, at higher reaction temperatures (27-37 °C) the corresponding apparent E_a values decreased to 39 ± 0.5 and 7 ± 0.5 kJ mol^{-1} for the two different St/Rh ratios (Table 1, Entries 2-4 and 6-8), reflecting increased mass transport limitation [12,44,45] as also found with the RhNP-TPPO@CCM-C system [35].

Recycling of the RhNP-TPPO@CCM-A latex was also evaluated for a series of reactions at a St/Rh ratio of 2000/1 (20 bar H_2, 25 °C, 0.25 h) with intermediate product extraction by diethyl ether (Figure 4). This extraction procedure is similar to that used to recycle the RhNP-TPP@CCM-C and RhNP-TPPO@CCM-C latexes [34,35], as well as the latex of a CCM-embedded molecular catalyst (Rh^{I}-TPP@CCM) [29,32]. A constant styrene conversion of *ca.* 18% (average TOF of ~1500 h^{-1} and *c*TOF of 3240 h^{-1}) and full EB selectivity were obtained over five reaction runs, but only when the catalyst system was reactivated with H_2 (20 bar, 1 h, 25 °C) prior to addition of a new batch of substrate. ICP-MS analyses of the product extracts showed only a cumulative loss of ~1.9% of the catalyst inventory after the five catalytic runs (SI, Table S4), thus confirming an effective confinement of the RhNPs in the TPPO@CCM-A micelles. Nevertheless, although the RhNP-TPPO@CCM-A latex yielded good recyclability and selectivity towards EB, the *c*TOF was much lower than for the previously examined

RhNP-TPPO@CCM-C system (6500 h^{-1}) [35] corroborating that the RhNP-TPPO@CCM-A catalyst is limited to a greater extent by mass transport of the substrate/product between the CCM-A cores and the organic bulk phase [12].

<Figure 4>

A TEM analysis of the recovered latex after the fifth run (SI, Figure S12), showed that the RhNPs remained well dispersed with a mean size (3.1 ± 0.6 nm) similar to that measured prior to catalysis (d_m = 3.1 ± 0.6 nm). However, a broader size distribution was obtained which shows a reorganization of the RhNPs, following a decrease of stabilization of the RhNPs in the CCMs.

The RhNP@CCM-A latex obtained from the TPPO-free CCM-A (SI, Figure S9) *via* a single-step procedure *(vide supra)* was also applied to the hydrogenation of styrene under the same reaction conditions as for initial RhNP-TPPO@CCM-A (*i.e.*, 20 bar H_2, 0.25 h, 25 °C, St/Rh ratio of 2000/1). Only <1% styrene conversion was here obtained, clearly emphasizing the key role of TPPO in the formation of efficiently confined and catalytically active RhNPs in the hydrophobic core of CCM-A, where the reaction takes place.

3.3.2. Acetophenone hydrogenation

The aqueous biphasic hydrogenation of acetophenone was also conducted with the one-pot synthesized RhNP-TPPO@CCM-A latex and further extended to encompass the RhNP-TPPO@CCM-C analog [35] (Table 2). Both catalysts selectively hydrogenated acetophenone to 1-phenyl-1-ethan-1-ol (PE) without formation of the ring-hydrogenated products 1-cyclohexylethan-1-one (CM) or 1-cyclohexylethan-1-ol (CE) at 25 and 60 °C and, as for styrene hydrogenation, the catalytic activity was higher for RhNP-TPPO@CCM-C (*c*TOF 3000 and 3880 h^{-1}; Table 1, Entries 1 and 2) than for RhNP-TPPO@CCM-A (*c*TOF 1506 and 3221 h^{-1}; Table 2, Entries 3 and 4) with the larger difference at the lower reaction temperature. This clearly indicates larger mass transport limitation in the latter system but also confirms that the cationic shell of the CCM does not block the acetophenone migration to the CCM core, which was previously suggested as a dominant cause of low activity using the analogous system with a TPP-functionalized core (RhNP-TPP@CCM-C) [32]. In perspective, this

facilitates the use of the CCM-A nanoreactors for a broader substrate scope as also shown with the CCM-C systems.

<Table 2>

4. Conclusion

Novel CCMs with polyanionic shells and TPPO-functionalized cores (TPPO@CCM-A) were synthesized with a spherical morphology and an average size of 45 nm by RAFT polymerization. The CCMs were used to prepare a catalytic RhNP-TPPO@CCM-A latex by a straightforward, one-pot procedure involving reduction of $[Rh(COD)(\mu\text{-}Cl)]_2$ carried in the micelle cores by toluene without auxiliary stabilizer or base. The nanocatalyst proved efficient (despite being hampered by some internal mass transfer limitation) and recyclable for the aqueous biphasic hydrogenation of both styrene and acetophenone, but yielded a lower activity compared to its CCM-C counterpart having a larger micelle size (*ca.* 98 nm) under identical reaction conditions. This suggests that the chemical nature of the anionic shell of the CCM-A makes the mass transport across the shell kinetically slower than for the CCM-C with a cationic shell for presently unknown reasons. Understanding such factors is key for tailoring the CCM polymeric systems and optimizing their catalytic performance, and such investigations will be a focal point of future work.

Acknowledgment

The authors thank the Technical University of Denmark, CNRS, and Université de Toulouse - Paul Sabatier for their support. Vincent Collière (CNRS, Laboratoire de Chimie de Coordination, Toulouse) is thanked for the TEM and STEM-HAADF analyses, as well as the Centre de Microcaractérisation Raimond Castaing, UAR 3623, Toulouse, France.

Funding Sources

This work has received funding from the European Union's Horizon 2020 research and innovation program under the Marie Skłodowska-Curie grant agreement No. 860322 (CCIMC project).

Contribution of Authors

Chantal J. Abou-Fayssal: Investigation, Visualization, Writing - Original Draft. **Leonhard Schill**: Investigation, Writing - Review & Editing. **Rinaldo Poli**: Funding acquisition, Conceptualization, Writing - Review & Editing. **Anders Riisager**: Conceptualization, Methodology, Resources, Supervision, Writing - Review & Editing. **Eric Manoury**: Conceptualization, Resources, Supervision, Writing - Review & Editing. **Karine Philippot**: Conceptualization, Resources, Supervision, Writing - Review & Editing.

Conflicts of Interest

The authors declare no conflict of interest.

Data Availability

The raw data required to reproduce these findings are available from the authors upon request.

References

[1] P. Serp, K. Philippot Editors, Nanomaterials in Catalysis Wiley-VCH (2012). Online ISBN:9783527656875. https://doi.org/10.1002/9783527656875

[2] D. Astruc (Ed.), Nanoparticles and Catalysis, Wiley-VCH, (2007). Online ISBN:978352762132.3 https://doi.org/10.1002/9783527621323

[3] B. Chaudret, K. Philippot, Organometallic nanoparticles of metals or metal oxides, Oil Gas Sci. Technol. 62 (2007) 799–817. https://doi.org/10.2516/ogst:2007062

[4] A. Roucoux, J. Schulz, H. Patin, Reduced transition metal colloids: A novel family of reusable catalysts?, Chem. Rev. 102 (2002) 3757–3778. https://doi.org/10.1021/cr010350j

[5] D. Astruc, F. Lu, J.R. Aranzaes, Nanoparticles as recyclable catalysts: The frontier between homogeneous and heterogeneous catalysis, Angew. Chem. Int. Ed. 44 (2005) 7852–7872. https://doi.org/10.1002/anie.200500766

[6] C. Burda, X. Chen, R. Narayanan, M.A. El-Sayed, Chemistry and properties of nanocrystals of different shapes, Chem. Rev. 105 (2005) 1025–1102. https://doi.org/10.1021/cr030063a

[7] J.L. Castelbou, E. Bresó-Femenia, P. Blondeau, B. Chaudret, S. Castillón, C. Claver, C. Godard, Tuning the selectivity in the hydrogenation of aromatic ketones catalyzed by similar ruthenium and rhodium nanoparticles, ChemCatChem 6 (2014) 3160–3168. https://doi.org/10.1002/cctc.201402524

[8] M. Guerrero, N.T.T. Chau, S. Noël, A. Denicourt-Nowicki, F. Hapiot, A. Roucoux, E. Monflier, K. Philippot, About the Use of Rhodium Nanoparticles in Hydrogenation and Hydroformylation Reactions, Curr. Org. Chem. 17 (2013) 364-399. https://doi.org/10.2174/1385272811317040006

[9] E. Guyonnet Bilé, R. Sassine, A. Denicourt-Nowicki, F. Launay, A. Roucoux, New ammonium surfactant-stabilized rhodium(0) colloidal suspensions: Influence of novel counter-anions on physico-chemical and catalytic properties, Dalton Trans. 40 (2011) 6524–6531. https://doi.org/10.1039/c0dt01763a

[10] E. Guyonnet Bilé, E. Cortelazzo-Polisini, A. Denicourt-Nowicki, R. Sassine, F. Launay, A. Roucoux, Chiral ammonium-capped rhodium(0) nanocatalysts: Synthesis, characterization, and advances in asymmetric hydrogenation in neat water, ChemSusChem 5 (2012) 91–101. https://doi.org/10.1002/cssc.201100364

[11] E. Guyonnet-Bilé, A. Denicourt-Nowicki, R. Sassine, P. Beaunier, F. Launay, A. Roucoux, N-Methylephedrium salts as chiral surfactants for asymmetric hydrogenation in neat water with rhodium(0) nanocatalysts, ChemSusChem 3 (2010) 1276–1279. https://doi.org/10.1002/cssc.201000206

[12] A. Borsla, A.M. Wilhelm, H. Delmas, Hydrogenation of olefins in aqueous phase, catalyzed by polymer-protected rhodium colloids: kinetic study, Catal. Today, 66 (2001) 389-395. https://doi.org/10.1016/S0920-5861(00)00635-0

[13] H. Mao, X. Liao, B. Shi, Amphiphilic tannin-stabilized Rh nanoparticles: A highly active and reusable catalyst in biphasic aqueous-organic system, Catal. Commun. 16 (2011) 210–214. https://doi.org/10.1016/j.catcom.2011.09.038

[14] C. Chaudhari, H. Imatome, Y. Nishida, K. Sato, K. Nagaoka, Recyclable Rh-PVP nanoparticles catalyzed hydrogenation of benzoic acid derivatives and quinolines

under solvent-free conditions, Catal. Commun. 126 (2019) 55–60. https://doi.org/10.1016/j.catcom.2019.02.019

[15] H. Hirai, M. Ohtaki, M. Komiyama, Preparation of Highly Active Hydrogenation Catalyst by Immobilization of Polymer-Protected Colloidal Rhodium Particles, Chem. Lett. 16 (1987) 149–152. https://doi.org/10.1246/cl.1987.149

[16] J.L. Castelbou, A. Gual, E. Mercadé, C. Claver, C. Godard, Ligand effect in the Rh-NP catalysed partial hydrogenation of substituted arenes, Catal. Sci. Technol. 3 (2013) 2828–2833. https://doi.org/10.1039/c3cy00388d

[17] C. Moreno-Marrodan, F. Liguori, E. Mercadé, C. Godard, C. Claver, P. Barbaro, A mild route to solid-supported rhodium nanoparticle catalysts and their application to the selective hydrogenation reaction of substituted arenes, Catal. Sci. Technol. 5 (2015) 3762–3772. https://doi.org/10.1039/c5cy00599j

[18] F. Martinez-Espinar, P. Blondeau, P. Nolis, B. Chaudret, C. Claver, S. Castillón, C. Godard, NHC-stabilised Rh nanoparticles: Surface study and application in the catalytic hydrogenation of aromatic substrates, J. Catal. 354 (2017) 113–127. https://doi.org/10.1016/j.jcat.2017.08.010

[19] C. Amiens, D. Ciuculescu-Pradines, K. Philippot, Controlled metal nanostructures: Fertile ground for coordination chemists, Coord. Chem. Rev. 308 (2016) 409–432. https://doi.org/10.1016/j.ccr.2015.07.013

[20] M.R. Axet, S. Castillón, C. Claver, K. Philippot, P. Lecante, B. Chaudret, Chiral diphosphite-modified rhodium(0) nanoparticles: Catalyst reservoir for styrene hydroformylation, Eur. J. Inorg. Chem. (2008) 3460–3466. https://doi.org/10.1002/ejic.200800421

[21] M. Ibrahim, M.M. Wei, E. Deydier, E. Manoury, R. Poli, P. Lecante, K. Philippot, Rhodium nanoparticles stabilized by ferrocenyl-phosphine ligands: Synthesis and catalytic styrene hydrogenation, Dalton Trans. 48 (2019) 6777–6786. https://doi.org/10.1039/c9dt01006h

[22] J.L. Pellegatta, C. Blandy, V. Collière, R. Choukroun, B. Chaudret, P. Cheng, K. Philippot. Catalytic investigation of rhodium nanoparticles in the hydrogenation of benzene and phenylacetylene. J. Mol. Cat. A Chem. 178 (2002) 55-61. https://doi.org/10.1016/s1381-1169(01)00298-9

[23] B. Cornils, W. A Herrmann, M. Beller, R. Paciello (Eds.), Applied Homogeneous Catalysis with Organometallic Compounds: A Comprehensive Handbook in Four

Volumes, Wiley-VCH (2017), ISBN: 9783527651733. https://doi.org/10.1002/9783527651733

[24] O. Nuyken, P.Persigehl, R. Weberskirch Amphiphilic Poly(Oxazoline)s - Synthesis and Application for Micellar Catalysis. Macromol. Symp. (2002) 163–173. https://doi.org/10.1002/1521-3900(200201)177:1<163::AID-MASY163>3.0.CO;2-W

[25] M. Niyaz Khan, Micellar Catalysis, CRC Press (2006), ISBN 9780429133749. https://doi.org/10.1201/9781420015843

[26] S. Chen, F. Gayet, E. Manoury, A. Joumaa, M. Lansalot, F. D'Agosto, R. Poli, Coordination Chemistry Inside Polymeric Nanoreactors: Interparticle Metal Exchange and Ionic Compound Vectorization in Phosphine-Functionalized Amphiphilic Polymer Latexes, Chem. Eur. J. 22 (2016) 6302–6313. https://doi.org/10.1002/chem.201504923

[27] A. Joumaa, F. Gayet, E.J. Garcia-Suarez, J. Himmelstrup, A. Riisager, R. Poli, E. Manoury, Synthesis of nixantphos core-functionalized amphiphilic nanoreactors and application to rhodium-catalyzed aqueous biphasic 1-octene hydroformylation, Polymers 12 (2020) 1107. https://doi.org/10.3390/POLYM12051107

[28] H. Wang, C. Fliedel, E. Manoury, R. Poli, Core-crosslinked micelles with a poly-anionic poly(styrene sulfonate)-based outer shell made by RAFT polymerization, Polymer 243 (2022) 124640. https://doi.org/10.1016/j.polymer.2022.124640

[29] H. Wang, L. Vendrame, C. Fliedel, S. Chen, F. Gayet, F. D'Agosto, M. Lansalot, E. Manoury, R. Poli, Triphenylphosphine-Functionalized Core-Cross-Linked Micelles and Nanogels with a Polycationic Outer Shell: Synthesis and Application in Rhodium-Catalyzed Biphasic Hydrogenations, Chem. Eur. J. 27 (2021) 5205–5214. https://doi.org/10.1002/chem.202004689

[30] H. Wang, L. Vendrame, C. Fliedel, S. Chen, F. Gayet, E. Manoury, X. Zhang, F. D'agosto, M. Lansalot, R. Poli, Core-Cross-Linked Micelles Made by RAFT Polymerization with a Polycationic Outer Shell Based on Poly(1-methyl-4-vinylpyridinium), Macromol. 53 (2020) 2198–2208. https://doi.org/10.1021/acs.macromol.9b02582

[31] S.S. Sambou, R. Hromov, I. Ruzhylo, H. Wang, A. Allandrieu, C. Sabatier, Y. Coppel, J.C. Daran, F. Gayet, A. Labande, E. Manoury, R. Poli, Amphiphilic polymeric nanoreactors containing Rh(I)-NHC complexes for the aqueous biphasic hydrogenation of alkenes, Catal. Sci. Technol. 11 (2021) 6811–6824. https://doi.org/10.1039/d1cy00554e

[32] H. Wang, A.M. Fiore, C. Fliedel, E. Manoury, K. Philippot, M.M. Dell'Anna, P. Mastrorilli, R. Poli, Rhodium nanoparticles inside well-defined unimolecular amphiphilic polymeric nanoreactors: Synthesis and biphasic hydrogenation catalysis, Nanoscale Adv. 3 (2021) 2554–2566. https://doi.org/10.1039/d1na00028d

[33] A.F. Cardozo, C. Julcour, L. Barthe, J.F. Blanco, S. Chen, F. Gayet, E. Manoury, X. Zhang, M. Lansalot, B. Charleux, F. D'Agosto, R. Poli, H. Delmas, Aqueous phase homogeneous catalysis using core-shell nanoreactors: Application to rhodium-catalyzed hydroformylation of 1-octene, J. Catal. 324 (2015) 1–8. https://doi.org/10.1016/j.jcat.2015.01.009

[34] C.J. Abou-Fayssal, C. Fliedel, R. Poli, A. Riisager, K. Philippot, E. Manoury, Confinement of Rh nanoparticles in triphenylphosphine oxide-2 functionalized core-crosslinked micelles for aqueous biphasic hydrogenation catalysis, Mater. Today Chem. 34 (2023) 101752. https://doi.org/10.1016/j.mtchem.2023.101752

[35] C.J. Abou-Fayssal, L. Schill, R. Poli, E. Manoury, K. Philippot, A. Riisager, One-pot Synthesis of Rh Nanoparticles in Polycationic-shell, Triphenylphosphine Oxide-functionalized Core-crosslinked Micelles for Aqueous Biphasic Hydrogenation, ChemCatChem (2024) e202400189. https://doi.org/10.1002/cctc.202400189

[36] F. D'Agosto, J. Rieger, M. Lansalot, RAFT-Mediated Polymerization-Induced Self-Assembly, Angew. Chem. Int. Ed. 59 (2020) 8368–8392. https://doi.org/10.1002/anie.201911758

[37] R.K. O'reilly, C.J. Hawker, K.L. Wooley, Cross-linked block copolymer micelles: Functional nanostructures of great potential and versatility, Chem. Soc. Rev. 35 (2006) 1068–1083. https://doi.org/10.1039/b514858h

[38] H. Wang, C.J. Abou-Fayssal, C. Fliedel, E. Manoury, R. Poli, Phosphine-Functionalized Core-Crosslinked Micelles and Nanogels with an Anionic Poly(styrenesulfonate) Shell: Synthesis, Rhodium(I) Coordination and Aqueous Biphasic Hydrogenation Catalysis, Polymers 14 (2022) 4937. https://doi.org/10.3390/polym14224937

[39] A.M. Fiore, V. Petrelli, C. Fliedel, E. Manoury, P. Mastrorilli, R. Poli, Acetate ion addition to and exchange in (1,5-cyclooctadiene)rhodium(I) acetate: relevance for the coagulation of carboxylic acid-functionalized shells of core-crosslinked micelle latexes, Dalton Trans. 52 (2023) 12534–12542. https://doi.org/10.1039/d3dt02260a

[40] N. Li, F. Chen, G. Wang, Q. Zeng, Copper-catalyzed C–P cross-coupling of arylmethyl quaternary ammonium salts via C–N bond cleavage, Monatsh. Chem. 151 (2020) 99–106. https://doi.org/10.1007/s00706-019-02535-y

[41] G.B. Deacon, J.H.S. Green, Vibrational spectra of ligands and complexes-II I&a-red spectra (3650-375 cm^{-1}) of triphenyl-phosphine, triphenylphosphine oxide, and their complexes, Spectrochim. Acta A 25 (1969) 355-364. https://doi.org/10.1016/0584-8539(69)80031-0

[42] S. Carenco, C. Boissière, L. Nicole, C. Sanchez, P. Le Floch, N. Mézailles, Controlled design of Size-tunable monodisperse nickel nanoparticles, Chem. Mater. 22 (2010) 1340–1349. https://doi.org/10.1021/cm902007g

[43] K. Senevirathne, A.W. Burns, M.E. Bussell, S.L. Brock, Synthesis and characterization of discrete nickel phosphide nanoparticles: Effect of surface ligation chemistry on catalytic hydrodesulfurization of thiophene, Adv. Funct. Mater. 17 (2007) 3933–3939. https://doi.org/10.1002/adfm.200700758

[44] Z.A. Piskulich, O.O. Mesele, W.H. Thompson, Removing the barrier to the calculation of activation energies: Diffusion coefficients and reorientation times in liquid water, J. Chem. Phys. 147 (2017) 134103. https://doi.org/10.1063/1.4997723

[45] H. Rafatijo, D.L. Thompson, General application of Tolman's concept of activation energy, J. Chem. Phys. 147 (2017) 224111. https://doi.org/10.1063/1.5009751

Figure and Scheme Captions

Scheme 1. Synthesis of the TPPO@CCM-A polymer.

Figure 1. DLS size distributions of aqueous dispersions of (a) the diblock R_0-(SS$^-$Na$^+$)$_{140}$-*b*-St$_{50}$-b-(St$_{0.9}$-co-SDPPO$_{0.1}$)$_{300}$-SC(S)SnPr, (b) TPPO@CCM-A in NaCl(aq) and (c) TPPO@CCM-A after core swelling with $CHCl_3$, NaCl/SS$^-$Na$^+$ ratio is 3.5. d) TEM image of the TPPO@CCM-A. Color coding: number (blue), volume (green), and intensity (red).

Figure 2. TEM image of one-pot synthesized RhNP-TPPO@CCM-A (left) and the corresponding size distribution (right) of RhNPs (d_m = 3.1 ± 0.6 nm).

Figure 3. Time plot for the aqueous biphasic hydrogenation of styrene using RhNPs-TPPO@CCM-A latex. Reaction conditions: styrene/Rh = 2000/1, 20 bar H_2, 25 °C.

Figure 4. Reuse of RhNPs-TPPO@CCM-A catalyst in five reaction runs of styrene hydrogenation with intermediate H_2 treatment (20 bar H_2, 25 °C, 1 h) and product extraction by diethyl ether. Reaction conditions: Styrene/Rh = 2000/1, 20 bar H_2, 25 °C, 0.25 h.

Schemes

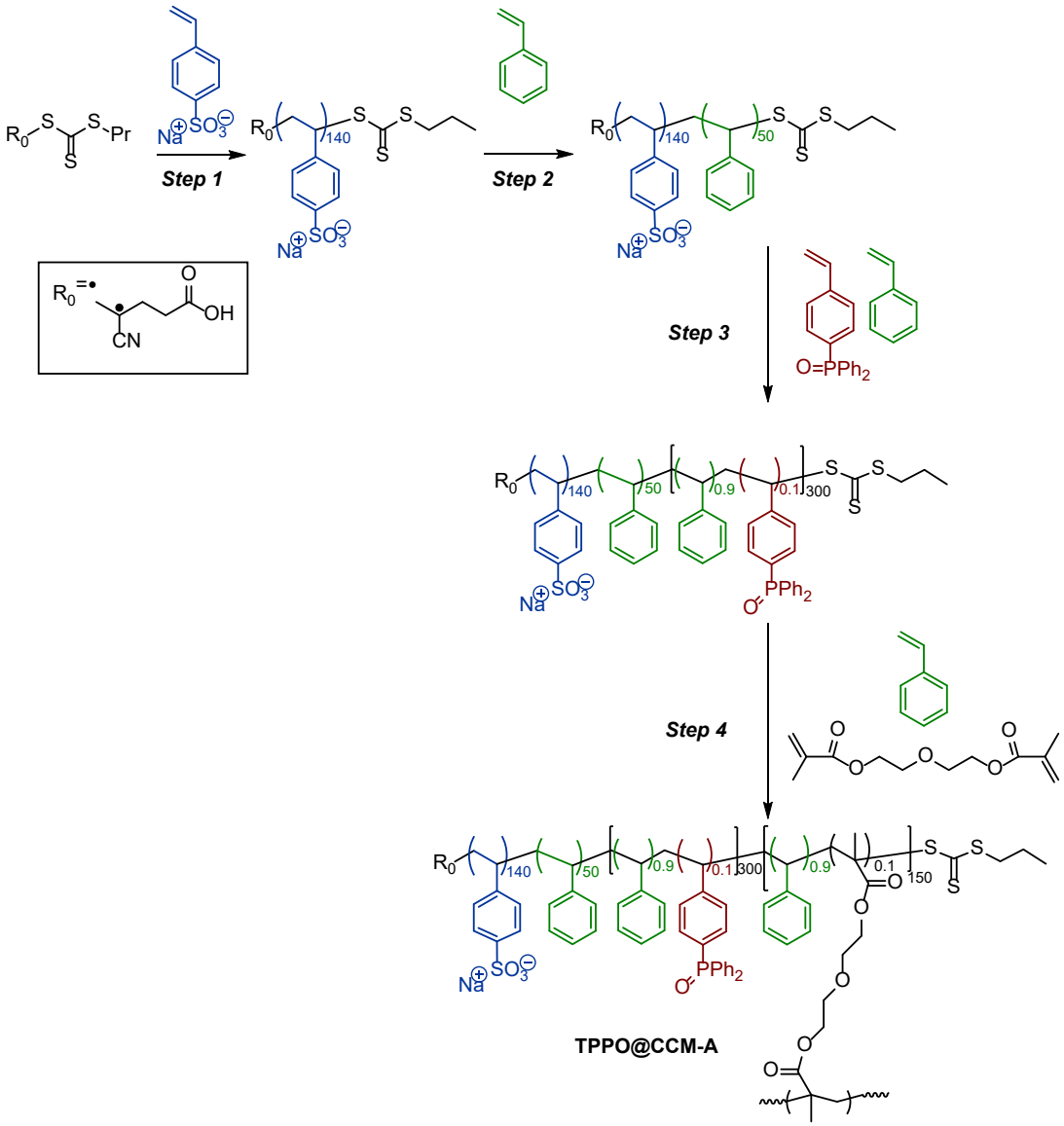

Scheme 1

Figures

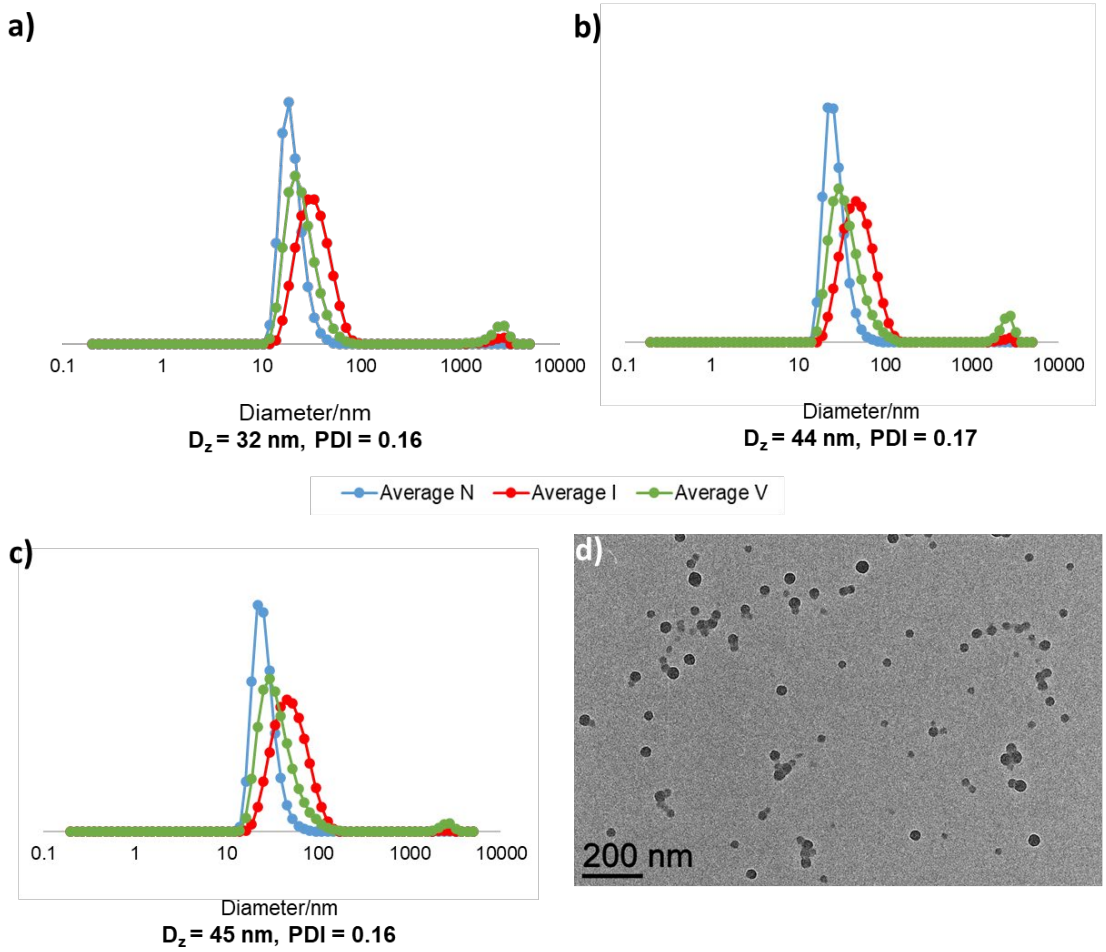

Figure 1

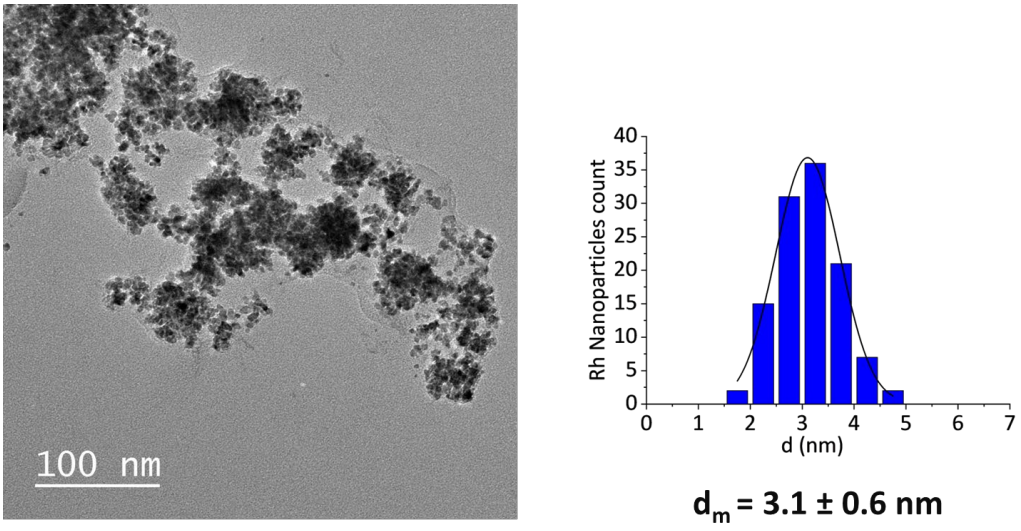

Figure 2

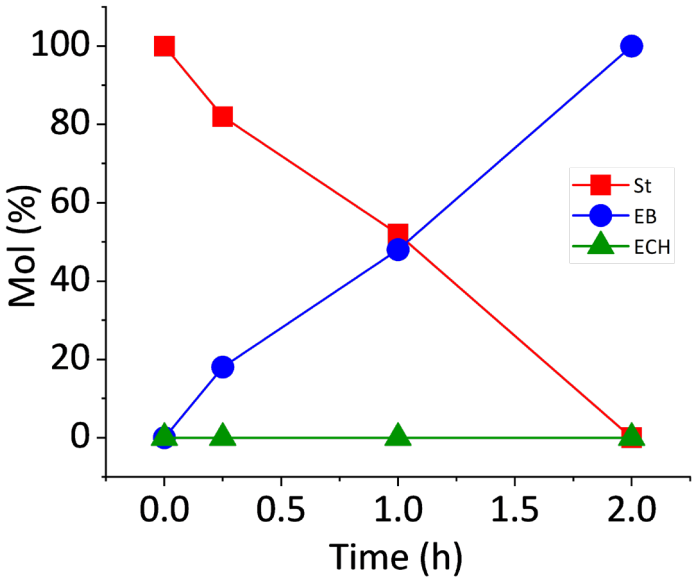

Figure 3

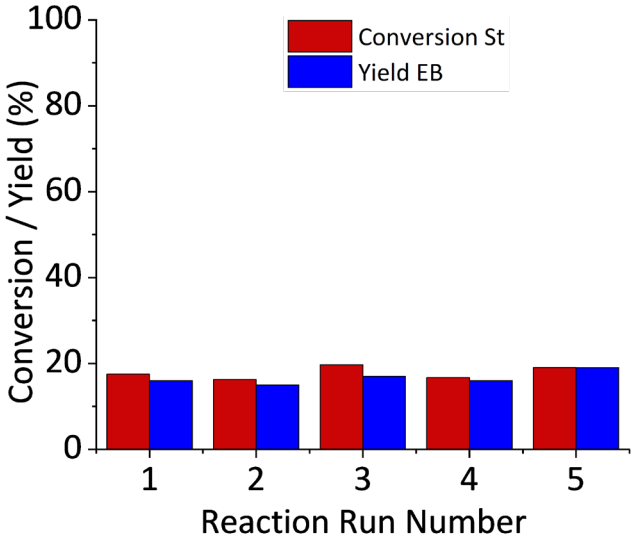

Figure 4

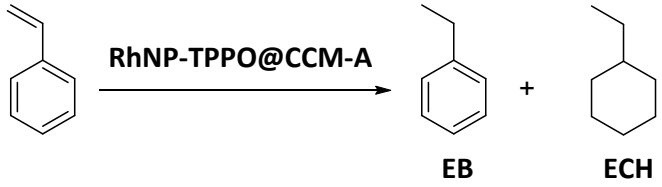

Table 1. Hydrogenation of styrene with RhNPs-TPPO@CCM-A latex.[a]

Entry	Molar styrene/Rh ratio	T (°C)	Conv. (%)	Selectivity (%)		TOF / *c*TOF (h^{-1})
				EB	ECH	
1	2000/1	24	17	>99	<0.1	1420 / 3250
2	2000/1	27	32	>99	<0.1	2735 / 6265
3	2000/1	31	36	>99	<0.1	2950 / 6750
4	2000/1	37	54	>99	<0.1	4375 / 10010
5	5000/1	24	13	>99	<0.1	2455 / 5620
6	5000/1	27	15	>99	<0.1	3055 / 6990
7	5000/1	31	17	>99	<0.1	3260 / 7470
8	5000/1	37	18	>99	<0.1	3415 / 7816

[a] Reaction conditions: 20 bar H_2, 0.25 h, 1200 rpm. EB: ethylbenzene, ECH: ethyl cyclohexane.

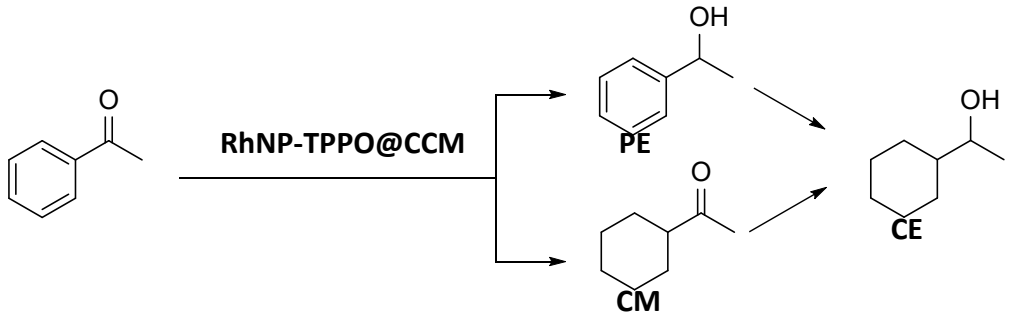

Table 2. Hydrogenation of acetophenone with RhNP-TPPO@CCM latexes.[a]

Entry	Catalyst	T (°C)	Conv. (%)	Selectivity (%)			TOF / *c*TOF (h^{-1})
				PE	CM	CE	
1	RhNP-TPPO@CCM-C	25	86	>99	<0.1	<0.1	2120 / 3000
2	RhNP-TPPO@CCM-C	60	>99	>99	<0.1	<0.1	2600 / 3880
3	RhNP-TPPO@CCM-A	25	45	>99	<0.1	<0.1	979 / 1506
4	RhNP-TPPO@CCM-A	60	60	>99	<0.1	<0.1	1407 / 3221

[a] Reaction conditions: Acetophenone/Rh = 5000/1, 20 bar H_2, 2 h, 1200 rpm.